

# Glucagon-Like Peptide 1 and Atrial Natriuretic Peptide in a Female Mouse Model of Obstructive Pulmonary Disease

Emilie Balk-Møller,<sup>1,2</sup> Johanne Agerlin Windeløv,<sup>1,2</sup> Berit Svendsen,<sup>2</sup> Jenna Hunt,<sup>2</sup> Seyed Mojtaba Ghiasi,<sup>2,3</sup> Charlotte Mehlin Sørensen,<sup>1</sup> Jens Juul Holst,<sup>1,2</sup> and Hannelouise Kissow<sup>1,2</sup>

<sup>1</sup>NNF Center for Basic Metabolic Research, Faculty of Health and Medical Sciences, University of Copenhagen, DK-2200 Copenhagen, Denmark; <sup>2</sup>Department of Biomedical Sciences, Faculty of Health and Medical Sciences, University of Copenhagen, DK-2200 Copenhagen, Denmark; and <sup>3</sup>Section for Cell Biology, Faculty of Science, University of Copenhagen, DK-2100 Copenhagen, Denmark

**ORCID numbers:** 0000-0002-9194-7886 (J. A. Windeløv); 0000-0002-3604-000X (B. Svendsen); 0000-0003-0508-7320 (J. Hunt); 0000-0001-8526-8513 (S. M. Ghiasi); 0000-0001-6853-3805 (J. J. Holst); 0000-0001-9351-8885 (H. Kissow).

Glucagon-like peptide-1 (GLP-1) is protective in lung disease models but the underlying mechanisms remain elusive. Because the hormone atrial natriuretic peptide (ANP) also has beneficial effects in lung disease, we hypothesized that GLP-1 effects may be mediated by ANP expression. To study this putative link, we used a mouse model of chronic obstructive pulmonary disease (COPD) and assessed lung function by unrestrained whole-body plethysmography. In 1 study, we investigated the role of endogenous GLP-1 by genetic GLP-1 receptor (GLP-1R) knockout (KO) and pharmaceutical blockade of the GLP-1R with the antagonist exendin-9 to -39 (EX-9). In another study the effects of exogenous GLP-1 were assessed. Lastly, we investigated the bronchodilatory properties of ANP and a GLP-1R agonist on isolated bronchial sections from healthy and COPD mice.

Lung function did not differ between mice receiving phosphate-buffered saline (PBS) and EX-9 or between GLP-1R KO mice and their wild-type littermates. The COPD mice receiving GLP-1R agonist improved pulmonary function ( $P < .01$ ) with less inflammation, but no less emphysema compared to PBS-treated mice. Compared with the PBS-treated mice, treatment with GLP-1 agonist increased ANP (*nppa*) gene expression by 10-fold ( $P < .01$ ) and decreased endothelin-1 ( $P < .01$ ), a peptide associated with bronchoconstriction. ANP had moderate bronchodilatory effects in isolated bronchial sections and GLP-1R agonist also showed bronchodilatory properties but less than ANP. Responses to both peptides were significantly increased in COPD mice ( $P < .05$ ,  $P < .01$ ).

Taken together, our study suggests a link between GLP-1 and ANP in COPD.

© Endocrine Society 2019.

This is an Open Access article distributed under the terms of the Creative Commons Attribution-NonCommercial-NoDerivs licence (<http://creativecommons.org/licenses/by-nc-nd/4.0/>), which permits non-commercial reproduction and distribution of the work, in any medium, provided the original work is not altered or transformed in any way, and that the work is properly cited. For commercial re-use, please contact [journals.permissions@oup.com](mailto:journals.permissions@oup.com)

**Key Words:** Glucagon-like peptide-1, atrial natriuretic peptide, lung disease, whole-body plethysmography, inflammation

Glucagon-like peptide-1 (GLP-1) is a peptide hormone secreted from the small and large intestine on meal intake (1, 2). It potentiates glucose-stimulated insulin secretion from pancreatic  $\beta$  cells and is therefore recognized as an incretin hormone (3). Owing to its glycemic

Abbreviations: ab, antibody; ANP, atrial natriuretic peptide; COPD, chronic obstructive pulmonary disease; ET-1, endothelin-1; EX-4, exendin-4; EX-9, exendin-9 to -39; GLP-1, glucagon-like peptide-1; GLP-1R, glucagon-like peptide-1 receptor; lira, liraglutide; LPS, lipopolysaccharide; OVA, ovalbumin; PenH, enhanced pause; qPCR, quantitative polymerase chain reaction; WT, wild-type.

and anorexic effects, GLP-1 receptor (GLP-1R) agonists are used for the treatment of type 2 diabetes and obesity (4). GLP-1 also has extrapancreatic effects including regulation of vascular tone and is thought to provide cardioprotection and neuroprotection (5-7). GLP-1 acts by binding to GLP-1R, which is found in the brain, heart, stomach, intestine, kidney, and nerves (6, 8-12). Additionally, several studies have shown the expression of GLP-1R in lung tissue (11, 13-18), which has motivated studies investigating a putative protective role of GLP-1 in lung disease in different rodent models (19-26). Viby et al showed that exogenous administration of the GLP-1R agonists liraglutide (lira) and exendin-4 (EX-4) improved lung function and reduced mortality in a mouse model of obstructive pulmonary disease (20). The improved lung function involved a decrease in enhanced pause (PenH), a measure of broncho-obstruction in mice, suggesting that GLP-1 might have bronchodilatory effects.

Interestingly, GLP-1 was recently linked to secretion of atrial natriuretic peptide (ANP) in a study published by Kim and colleagues. They demonstrated that GLP-1 reduced blood pressure by stimulating the release of ANP (12). The main function of ANP is to lower blood pressure by a number of actions in the kidney, where it increases vascular permeability, induces vasorelaxation, and causes natriuresis (27). Furthermore, ANP inhibits the production of aldosterone by actions in the adrenal glands and induces vasorelaxation of vascular smooth muscle cells in general (28-33). ANP may also be secreted from cells in the lung (33, 34) and some studies have shown a direct relaxant effect of ANP on isolated bronchi from guinea pigs and cows (35-37). A role of ANP in human lung diseases has also been investigated, and increased levels of ANP have been reported in adult respiratory distress syndrome (38) as well as in patients with chronic obstructive pulmonary disease (COPD) (39). Furthermore, in patients with asthma, ANP infusions have had bronchodilatory effects (40). Taken together, this suggests that ANP may exert direct beneficial effects on the bronchi that could improve lung function in disease states. Little is known, however, about the underlying mechanisms, including whether the actions of GLP-1 and ANP might be associated.

In the present studies, our major aim was to evaluate the potential effect of endogenous GLP-1 during pulmonary disease. We induced GLP-1 signaling deficiency by either blocking GLP-1R pharmacologically (with EX-9) or by genetic deletion of the GLP-1R and subjected these animals to a mouse model of COPD (20). Our main end point was lung function, which was measured in a whole-body plethysmograph with PenH as a measurement of bronchoconstriction. In addition, we analyzed (by quantitative polymerase chain reaction [qPCR]) the expression of key candidate genes in lung disease, including *nppa* and ANP receptors (*npr1* and *npr3*) in COPD mice treated with GLP-1R agonists. We also performed direct measurements of the bronchodilatory effects of ANP and GLP-1R agonists on isolated bronchi of healthy and COPD mice. Because of the reported anti-inflammatory effects of GLP-1 in the lung (41-43), we additionally investigated whether the protective effect of exogenous GLP-1R agonists could be mediated by attenuation of inflammation.

## 1. Methods

### A. Animals

All experiments were conducted in accordance with internationally accepted principles for the care and use of laboratory animals, and the animal studies were approved by the Danish Animal Experiments Inspectorate (2013-15-2934-00833). Ten-week-old BALB/c and C57BL/6JRj female mice weighing approximately 20 g were obtained from Janvier Labs (Saint Berthevin).

Mice were housed in air-conditioned (21°C) and humidity-controlled (55%) rooms with a 12-hour light, 12-hour dark cycle with free access to food and water.

The constitutive knockout (KO) mouse for GLP-1R (*Glp1r* KO) was generated deleting exons 4 and 5 of the *Glp1r* gene on Cre expression. We purchased the conditional KO for the *Glp1r* gene from the MRC Harwell Institute (C57BL/6N-Glp1rtm1c(KOMP)MbpH) (44). In this mouse, exons 4 and 5 are flanked by LoxP sites. This conditional model was bred

to cytomegalovirus-Cre (45), which expresses Cre recombinase ubiquitously, resulting in a constitutive KO allele for *Glp1r* (*Glp1r* (f/f) × Cre). All animals were bred by heterozygote crossing. The offspring were genotyped by PCR on genomic DNA extracted from ear snips using optimized primers (Table 1).

Wild-type (WT) littermates (*Glp1r* (+/+) × Cre) were used as control animals in all experiments. All genetically modified animals used in the experiments were female, 10 ± 1-week-old, and generation N3 to N4.

Before experiments were initiated the strain was validated by showing lack of insulin secretion from the pancreatic β cells on stimulation with GLP-1 in the KO mice in an isolated perfused pancreas preparation. We also validated the mice by the absence of GLP-1R antibody (ab) immune reactivity.

### B. Isolated Perfused Mouse Pancreas

Pancreas perfusions were performed as previously described (46). In short, the mice were anesthetized with intraperitoneal injection of ketamine (90 mg/kg Ketaminol vet, MSD Animal Health) and xylazine (10 mg/ml, Rompun vet, Bayer Animal Health).

The stomach, kidney, and spleen were tied off. Proximally to the celiac artery, the aorta was ligated, and a catheter was inserted in the aorta thereby providing arterial perfusion with a modified Krebs-Ringer bicarbonate buffer (in mM: 118.3 NaCl, 3.0 KCl, 2.6 CaCl<sub>2</sub>·2H<sub>2</sub>O, 1.2 KH<sub>2</sub>PO<sub>4</sub>, 1.2 MgSO<sub>4</sub>·2H<sub>2</sub>O, 25.0 NaHCO<sub>3</sub>, 10 glucose, 0.1% bovine serum albumin, 5% dextran) (Pharmacosmos). Effluent samples were collected through a portal vein catheter every minute. The perfusion system (UP-100 universal perfusion system, Hugo Sachs Electronic) had a constant flow of 1 mL/min, perfusion buffer was maintained at 37°C, oxygenated with 95% O<sub>2</sub> to 5% CO<sub>2</sub>, and perfusion pressure (40-50 mmHg) was monitored throughout the experiment. GLP-1R KO mice or WT littermates (n = 8) were stimulated for 10 minutes with 0.1 nM and 1.0 nM GLP-1 7-36 amide (Bachem) at 15 and 40 minutes, respectively. At the end of the experiments, L-arginine was added as a positive control (10 mM).

Insulin concentrations in venous effluents were quantified by use of an in-house radioimmunoassay, employing ab code 2006-3 (47, 48).

**Table 1. Table of Primers Used for Genotyping and Gene Expression Analysis**

Cre	F	GCC TGC ATT ACC GGT CGA TGC AAC GA
	R	GTG GCA GAT GGC GCG GCA ACA CCA TT
Murine GLP-1r 5'arm WT	F	GGAGGATAGGACATAGTCCCAAA
Murine GLP-1r Crit WT	R	CCCAGCCACTCTCAGCTATT
Murine GLP-1r 5'mut	R	GAACTTCGGAATAGGAACCTCG
Murine GLP-1r 5'CAS	F	AAGGCGCATAACGATACCAC
	R	CCGCCTACTGCGACTATAGAGA
Murine GLP-1r 3'LOXP	R	ACTGATGGCGAGCTCAGACC
ANP ( <i>nppa</i> )	F	TGCCGGTAGAAGATGAGGTC
	R	AGCCCTCAGTTTGCTTTTCA
ANPR-A ( <i>npr1</i> )	F	AAGAGACGATGGGCAGGATA
	R	CACTGCCTGGACATAGAGCA
ANPR-C ( <i>npr3</i> )	F	TGACACCATTTCGGAGAATCA
	R	TTTCACGGTCCTCAGTAGGG
ET-1 ( <i>edn1</i> )	F	CTGCCAAGCAGGAAAAGAAC
	R	TTGTGCGTCAACTTCTGGTC
Apelin ( <i>apl</i> )	F	ATGAATCTGAGGCTCTGCGTGCAG
	R	TTAGAAAGGCATGGGGCCCTTATG
E-selectin ( <i>sele</i> )	F	CGCCAGAACAACAATTCCAC
	R	ACTGGAGGCATTGTAGTACC
Hypoxanthine phosphoribosyltransferase 1 ( <i>hprt-1</i> )	F	AAGCTTGCTGGTGAAAAGGA
	R	GGCTTTGTATTGGCTTTTCC

Abbreviations: F, forward; R, reverse.

### C. Mouse Model of Chronic Obstructive Pulmonary Disease

To induce development of a COPD-like phenotype, we used a model (20) that combines elements from an ovalbumin (OVA)-induced asthma model and a model of lipopolysaccharide (LPS)-induced COPD (20). Mice were injected subcutaneously (s.c.) with 0.1 mL homogenized heat-coagulated hen's egg white. After a 14-day sensitization period, the animals were subjected to aerosolized OVA (20 mg/mL; Sigma-Aldrich) on days 14 and 16 and aerosolized LPS from *Escherichia coli* O55:B55 (2.5 mg/mL; Lot No. 057M4013V, Sigma-Aldrich) on days 15 and 17 in an exposure chamber (Buxco). In both cases, compounds were delivered at an air flow rate of 2 L/min for 30 minutes with OVA and 15 minutes with LPS.

### D. Determination of Lung Function

Lung function measurements were carried out using a whole-body plethysmograph (Emka Technologies) for unrestrained rodents. Bronchoconstriction was measured indirectly by PenH measurements, which is a calculated composite index indicative of airway obstruction based on changes in breathing patterns as a result of bronchoconstriction (49).  $\text{PenH} = \text{PEP} / \text{PIP} \times \text{pause}$ , ( $\text{pause} = \text{Te} - \text{Tr} / \text{Tr}$ ), where PEP is the peak expiratory pressure, PIP is the peak inspiratory pressure, Te is the time of expiration, and Tr is the relaxation time, which is the time needed for the pressure decay to reach 36% of the total expiratory pressure signal. PenH values less than 1 are considered normal.

Animals were measured once daily from day 12. On day 18, the animals were measured at exactly 12, 14, and 16 hours after the last LPS inhalation. Data are presented as time-effect plots and as bar graphs showing PenH values at day 18, 12 hours after the last LPS inhalation. Statistics were carried out using 1-way analysis of variance (ANOVA) in GraphPad Prism version 7.

### E. Optimization of the Model

We first investigated the responsiveness to COPD induction in 2 widely used mouse strains: BALB/c and C57BL/6JRj with and without sensitization with an OVA pellet injected s.c. (50, 51). Next, we investigated the duration of the response in C57BL/6JRj mice by exposing 1 group of mice ( $n = 8$ ) to LPS in the morning followed by measurements every 2 hours during the day, and the other group ( $n = 8$ ) was exposed in the evening and evaluated the following day. PenH peaked 10 to 12 hours after the last LPS inhalation but after 30 hours PenH was less than 1. Based on this, we continued our experiments with C57BL/6JRj mice, which were either euthanized in the peak period at 12 hours (referred to as the “12-h” group in the remaining text) or 72 hours after last LPS inhalation (referred to as the “72-h” group from here on). Data from the optimization experiments are found in Fig. 1.

### F. Chronic Obstructive Pulmonary Disease Model

In the first experiment, 48 C57BL/6JRj mice were divided into 3 groups receiving lira, EX-9, or PBS. Plethysmograph measurements were performed for 3 minutes, and the animals were humanely killed 12 or 72 hours after last LPS inhalation.

In the next experiment, GLP-1R KO mice and WT littermates ( $n = 30$ ) had COPD induced and plethysmography was performed as above. Mice were humanely killed 12 or 72 hours after last LPS inhalation.

For statistical analysis of differences in PenH between groups, 1-way ANOVA followed by Bonferroni post hoc test was used.

### G. Peptides

Animals received s.c. injections twice daily (8:00 AM and 3:00 PM) with the GLP-1 analogue lira (Novo Nordisk) at a dose of 0.6 mg daily. Lira is a long-acting GLP-1 analogue due to

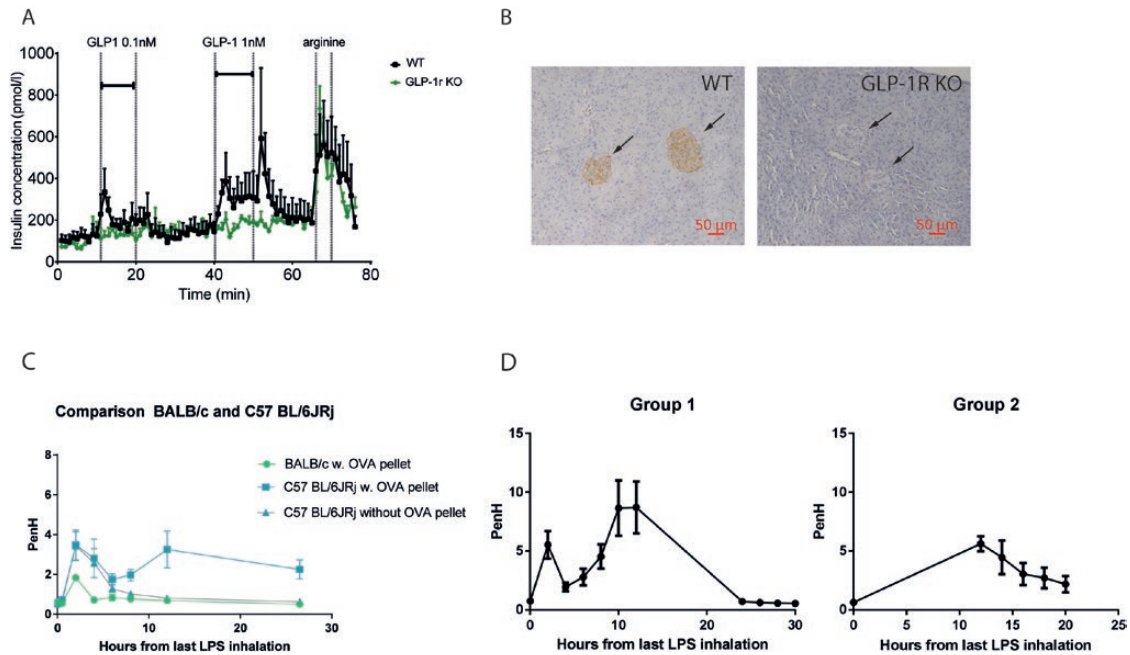


**Figure 1.** Validation of KO mouse strain and optimization of COPD model. A, Insulin secretion on GLP-1 stimulation by the pancreas using isolated pancreas perfusion. As opposed to the WT mice (black), the KO mice (green) do not respond to GLP-1. B, Immunohistochemical staining with GLP-1 R ab of pancreatic islets in (left) WT and (right) GLP-1R KO mice. Arrows point to pancreatic  $\beta$  cells in the islets of Langerhans but no immunoreaction in the GLP-1 R KO mouse. C, Comparison of responses to COPD-induction in BALB/c mice and C57BL/6JRj with and without sensitization with OVA pellets. D, Investigation of the duration and intensity of the response to COPD induction in C57BL/6JRj mice. Group 1 was measured from time 0 to 12 and 24 to 30 hours after the last LPS inhalation, and group 2 was measured from 12 to 24 hours.

acylation and in the body is bound to albumin for a slow release; therefore, this compound was used for the *in vivo* experiments (52). To antagonize the GLP-1R we used GLP-1 (9-39) (EX-9) (53) (4 017 799.1000, H8740, Bachem) at a dose of 0.2 mg daily or PBS as control. Treatments were all started at day 10 after sensitization and continued until animals were humanely killed. Doses were chosen based on previous experiments (20).

ANP (A8208, Sigma-Aldrich) and exendin-4 (EX-4) (Caslo) for wire myography was dissolved in double-distilled  $H_2O$ . EX-4 is a 39 AA peptide with 50% homology to GLP-1 (54) that is not influenced by variable protein binding. Therefore this compound was used for the *in vitro* experiments.

### H. Histopathology and Immunohistochemistry

Histopathology was carried out on the 4 groups: lira/PBS 12-h and lira/PBS 72-h ( $n = 32$ ). The lungs were fixed by instillation of 4% paraformaldehyde through the trachea immediately after death. The lungs were removed from the cavity and placed in 4% paraformaldehyde for 24 to 48 hours. Next, the lungs were embedded in paraffin and 4- $\mu$ m sections were cut and dried (60°C, 1 hour). Paraffin was removed with Histo-Clear (National Diagnostics, BioNordika) and sections were rehydrated in alcohol.

Sections stained with hematoxylin (Sigma-Aldrich) and eosin (Sigma-Aldrich) were used for histological investigation, and sections stained with periodic acid–Schiff (Sigma-Aldrich) were used for scoring of goblet cell metaplasia.

Antigen retrieval was achieved by boiling (microwave 20 minutes) in EDTA buffer pH 9 (TA-125-PM4X, Thermo Fisher) for GLP-1R staining and citrate buffer pH 6 (TA-125-PM1X,

Thermo Fisher) for staining of pulmonary macrophages. UltraVision Quanto Mouse on Mouse Detection Systems (TL-060-QHDM, Thermo Fisher) was used following provided instructions. The primary antibodies used were GLP-1R ab clone 7F38-s (55,56,57) diluted 1:50 and mannose receptor ab (58) diluted 1:12 000.

Semiquantitative histopathological scoring was carried out blinded based on the study by Zeldin et al (59). Scores were based on perivascular edema, perivascular/peribronchial acute inflammation, goblet cell metaplasia of the bronchioles, and macrophages/mononuclear cells in the alveolar spaces.

Statistical analysis of the inflammation scores was carried out using 1-way ANOVA followed by Bonferroni post hoc test comparing lira 12-h with PBS 12-h and lira 72-h with PBS 72-h.

### I. Inflammatory Markers

Blood was collected from the vena cava into EDTA-coated Eppendorf tubes before death and was directly centrifuged ( $1000 \times g$ , 10 minutes,  $4^{\circ}\text{C}$ ). Plasma was transferred into fresh Eppendorf tubes and was immediately placed on ice until storage at  $-20^{\circ}\text{C}$ . Plasma concentrations of 10 different proinflammatory cytokines were measured using a multispot assay system (Cat. No. K15048D, Meso Scale) according to the manufacturer's instruction. The assay quantified interferon- $\gamma$ , interleukin (IL)-1 $\beta$ , IL-2, IL-4, IL-5, IL-6, IL-10, IL-12p70, KC/GRO, and tumor necrosis factor (TNF)- $\alpha$ .

### J. Real-Time Reverse Transcriptase Quantitative Polymerase Chain Reaction

Total RNA was extracted using the Nucleo-Spin kit (740955, Macherey-Nagel) according to the manufacturer's instructions. Quality of the extracted RNA was assessed from absorbance measurements using a NanoDrop-1000 machine (Thermo Scientific). A total of 500 ng total RNA was used for complementary DNA (cDNA) synthesis with the iScript-cDNA Kit (1708891, BioRad). Real-time reverse transcriptase quantitative polymerase chain reaction was performed on 12 ng cDNA with SybrGreen PCR mastermix (Life Technologies) using specific primers and run in a real-time PCR machine (Applied Biosystems). Gene expression levels were normalized to the reference gene *Hprt1* (60) using the  $-\Delta\text{Ct}$  method. For simplicity, data are presented in the figures as fold-change values, which were calculated by the  $\Delta\Delta\text{Ct}$  method. Target genes were ANP (*nppa*), ANPR-A (*npr1*), ANPR-C (*npr3*), endothelin-1 (*end1*), apelin (*apln*), and E-selectin (*sele*). Primer sequences are shown in Table 1. In addition to the COPD mice, we added 2 groups of healthy animals that were not exposed to COPD induction but received lira (0.6 mg daily) or PBS for 10 days. This group was considered "healthy" and used for comparison of messenger RNA expression levels in healthy and COPD mice. Statistics were carried out on  $\Delta\text{Ct}$  values using 1-way ANOVA followed by Bonferroni post hoc test.

### K. Wire Myography

Mice were humanely killed by cervical dislocation and the entire lung was carefully removed and placed in Krebs Ringer bicarbonate solution (in mM: 118.3 NaCl, 4.7 KCl, 1.2  $\text{MgSO}_4$ , 1.2  $\text{KH}_2\text{PO}_4$ , 25  $\text{NaHCO}_3$ , 2.5  $\text{NaHCO}_2$ , 2.5 CaCl, and 10 glucose, pH 7.35-7.45) (61). The trachea and main bronchi were isolated using a dissection microscope, and sections of 1 to 2 mm were cut from the main left and main right bronchus in close proximity to the bifurcation. The sections were mounted by threading them on 2 steel wires (40  $\mu\text{m}$  diameter). Sections were placed in a wire myograph chamber (Danish Myo Technology) filled with 7 mL Krebs-Ringer bicarbonate buffer ( $37^{\circ}\text{C}$  and oxygenated with 95%  $\text{O}_2$  to 5%  $\text{CO}_2$  to maintain pH) and secured to 2 supporters. One of the supporters was attached to a micrometer, allowing control of ring circumference, and the other supporter was attached to a force transducer for measurements of isometric contraction. Tension was applied to the sections and the tissue

was left to equilibrate at resting tension for 1 hour before stretching to 3 mN for mice and 5 mN for rats. Buffer was replaced every 30 minutes. Tissue responses (contraction) were measured in response to addition of potassium physiological saline solution buffer, rich in KCl (in mM: 74.7 NaCl, 60 KCl, 1.18  $\text{KH}_2\text{PO}_4$ , 1.17  $\text{MgSO}_4 \cdot 6\text{H}_2\text{O}$ , 14.9  $\text{NaHCO}_3$ , 0.0026 EDTA, 1.6  $\text{CaCl}_2 \cdot 2\text{H}_2\text{O}$ , 5.5 glucose). In the absence of proper contraction, the sections were further stretched in increments of 2 mN until a significant response to the potassium physiological saline solution was observed. In a pilot experiment, a dose-response curve to carbachol was established ( $1 \times 10^{-10}$  to  $1 \times 10^{-3}$  M) to identify the concentration of carbachol resulting in a submaximal response approximately 80% of the maximum achievable. The desired submaximal contraction occurred at a concentration of  $1 \times 10^{-7}$  M, and this was used for subsequent studies testing the effects of either ANP or EX-4.

The bronchial rings were precontracted with carbachol (0.1  $\mu\text{M}$ ) and allowed to stabilize for 15 minutes before ANP or EX-4 was added in a cumulative fashion at 10-fold increases (0.001-1.0  $\mu\text{M}$ ) separated by 20 minutes between additions. At the end of each protocol, 0.1  $\mu\text{M}$  sodium nitroprusside (SNP; positive control) was added to relax the tissue completely and provide a standard ( $R_{\text{max}}$ ) to which the relaxation of each peptide was compared. The dilation by SNP was expressed as the percentage of precontraction with carbachol. Wire myography was also carried out in bronchi of C57BL/6JRj COPD mice. Experiments were carried out 72 hours after the last LPS inhalation.

Statistics analyzing the effects of ANP and EX-4 at different concentrations were carried out by 1-way ANOVA followed by Bonferroni post hoc test comparing each concentration to 0.001  $\mu\text{M}$ , which is considered as zero effect. Comparisons between sick and healthy animals were analyzed by 2-way ANOVA followed by Sidak post hoc test comparing the 2 groups at each concentration.

## 2. Results

### A. Validation of the Glucagon-like Peptide-1 Receptor Knockout Strain

We generated a GLP-1R KO strain for this study and validated the strain functionally for the loss of GLP-1R activity by investigating GLP-1-induced potentiation of glucose-stimulated insulin secretion from isolated perfused mouse pancreas. Stimulation with 0.1 nM and 1.0 nM GLP-1 had no effects in GLP-1R KO mice but increased insulin secretion in WT littermates (Fig. 1A). Furthermore, we investigated the lack of GLP-1R expression by immunohistochemistry using a GLP-1R ab on pancreatic islets. As expected, there was no visible staining of the pancreatic  $\beta$  cells in GLP-1R KO mice, whereas WT littermates showed a normal staining pattern (Fig. 1B).

### B. Optimization of the Chronic Obstructive Pulmonary Disease Model

We found C57BL/6JRj to be more responsive to induction of COPD-like phenotype than BALB/c mice (Fig. 1C). Sensitization with an OVA pellet of C57BL/6JRj mice before OVA and LPS treatment resulted in a second peak in PenH values and prolonged the entire response compared to the nonsensitized mice (Fig. 1C). Indeed, if mice were not sensitized, the obstruction was over in less than 12 hours compared to 30 hours in sensitized mice. PenH values reached a maximum between 10 to 12 hours after the last LPS inhalation and were back to normal ( $\text{PenH} < 1$ ) after 24 hours (Fig. 1D). Having gained this insight, we measured PenH in all animals in subsequent experiments precisely 12, 14, and 16 hours after the last LPS inhalation, when lung disease was considered to be most severe.

### C. Endogenous Glucagon-Like Peptide-1 Is not Protective in Lung Disease

When measuring lung function in COPD mice, we found no significant difference between the EX-9- and PBS-treated groups regarding PenH at 12 hours after the last LPS inhalation,

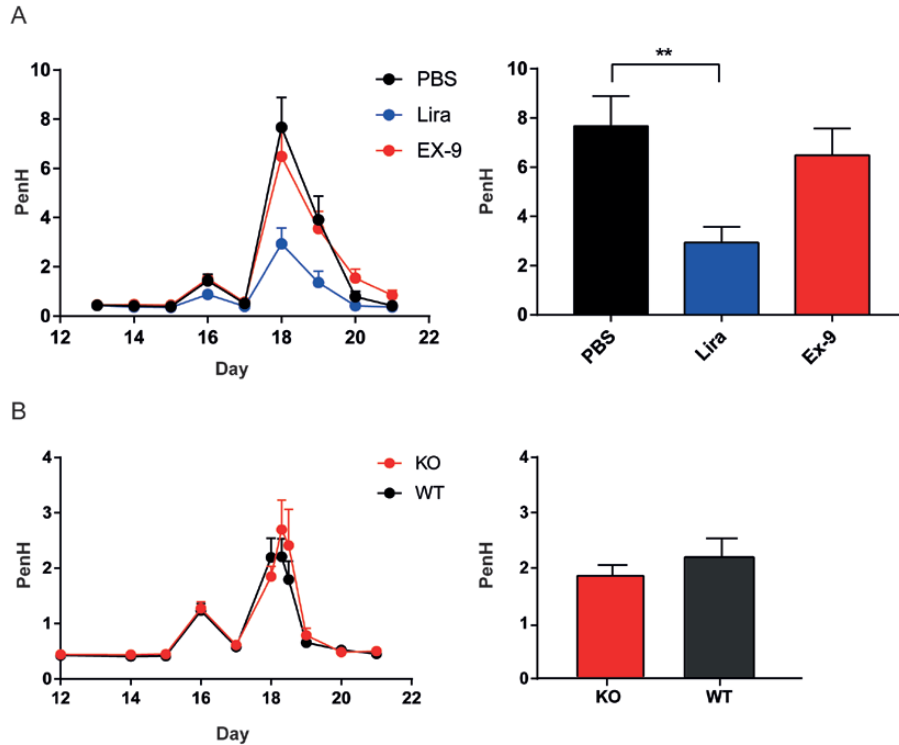


**Figure 2.** Endogenous GLP-1 is not protective in COPD. Data are presented as time-effects plots from day 12 to 21 in the left panel. Right panel shows bar graphs at day 18, 12 hours after the last LPS inhalation. A, Study investigating the effect on PenH by antagonizing the GLP-1R with EX-9,  $n = 48$ . B, GLP-1R KO and WT,  $n = 30$ . Data are shown as means  $\pm$  SEM. Statistics were carried out with 1-way ANOVA followed by Bonferroni post hoc test.  $**P < .01$

whereas there was a significant decrease in PenH in the lira group compared to the PBS group ( $P < .01$ ) (Fig. 2A).

We found no difference in PenH between the GLP-1R KO and WT littermates (Fig. 2B), supporting the lack of effect of endogenous GLP-1.

#### D. Effect of Liraglutide on Histopathology and Inflammatory Markers in Chronic Obstructive Pulmonary Disease

The histopathological score was significantly decreased in the lira 12-h group compared to the PBS 12-h group ( $P < .05$ ). In mice killed 72 hours after last LPS inhalation there was no difference between groups (Fig. 3A-3E). We found no difference with respect to the development of emphysema between the groups receiving PBS or lira (Fig. 3F). Also, we found no difference in plasma concentrations of interferon- $\gamma$ , IL-1 $\beta$ , IL2, IL-4, IL-5, IL-6, IL-10, IL-12p70, KC/GRO, and TNF- $\alpha$  between groups (PBS/lira 12-h and PBS/lira 72-h) (Fig. 2K). IL-1 $\beta$ , IL-4, and IL-12p70 were all less than the detection limit according to the quality control from the manufacturer.

#### E. Gene Expression Analysis

Lung tissue was isolated from the 4 groups PBS/lira 12-h and PBS/lira 72-h from COPD mice and from healthy mice treated with lira or PBS but not subjected to the COPD model.

Transcripts of *nppa* were increased more than 10-fold in the lira 72-h group compared to the PBS 72-h group ( $P < .01$ ) (Fig. 4A) and markedly increased when compared to the healthy lira group ( $P < .001$ ). The expression of the ANP receptor *npr1* was increased 16-fold in the PBS 12-h group compared to the lira 12-h group ( $P < .001$ ) (Fig. 4B).



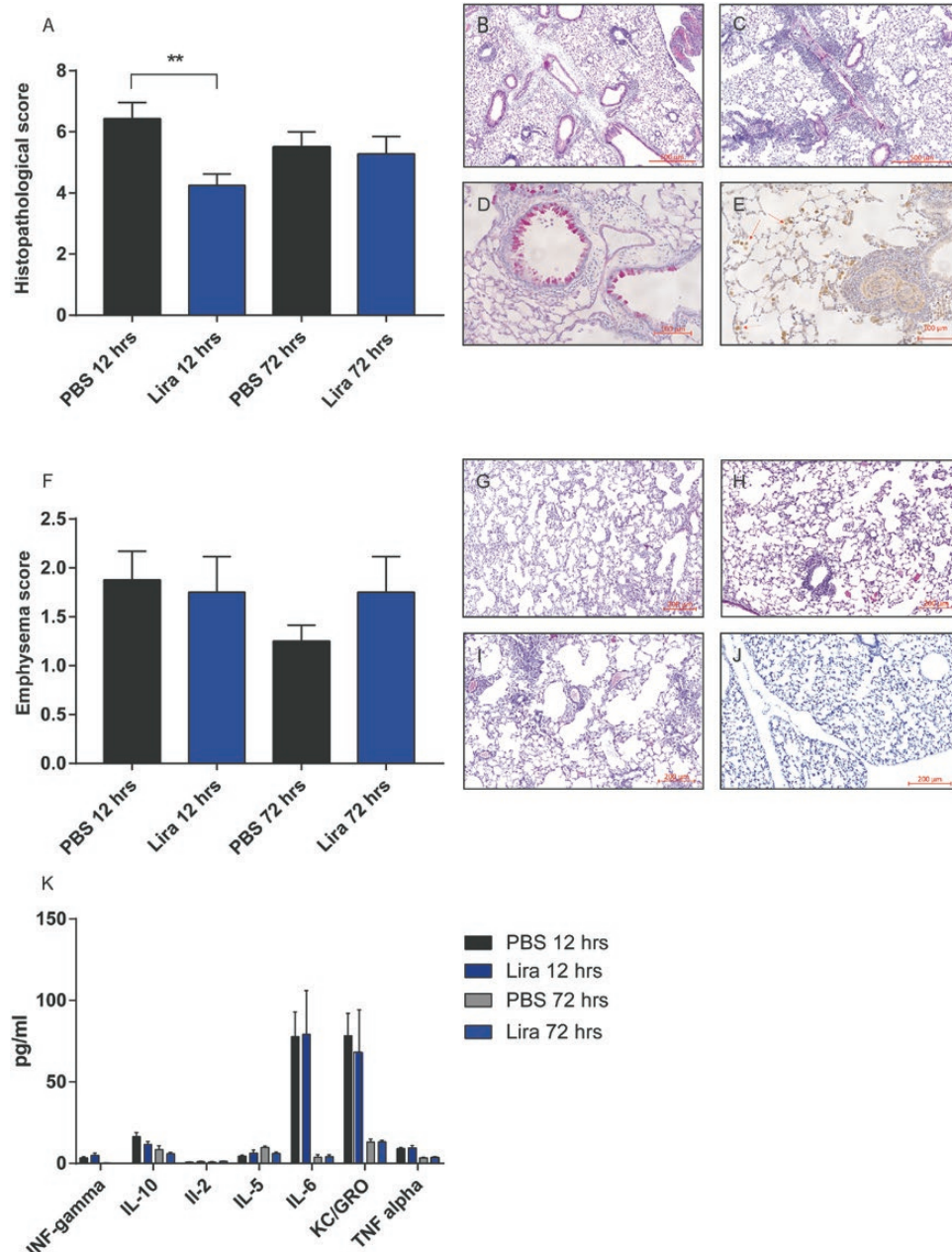


**Figure 3.** Effect of liraglutide on histopathology and inflammatory markers in COPD. A, Bar graph of histopathological score in the different groups. H&E staining showing B, perivascular edema; C, perivascular/peribronchial acute inflammation; D, goblet cell metaplasia of the bronchioles; and E, macrophages/mononuclear cells in the alveolar spaces. F, Emphysema score. Examples of emphysema scored as G, mild; H, moderate; I, and severe. J, Healthy mouse lung for comparison. K, Measurements of proinflammatory cytokines in plasma from COPD mice. Comparisons were carried out between lira 12-h and PBS 12-h, lira 72 h and PBS 72 h. Data are shown as means  $\pm$  SEM,  $n = 32$ . Statistics were analyzed by 1-way ANOVA followed by Bonferroni post hoc test.  $**P < .01$ .

The clearance receptor for ANP, *npr3*, was upregulated by a factor of 2 in the 72-h PBS group compared to the 72-h PBS group ( $P < .05$ ). Surprisingly, the healthy lira group expressed 16-fold more *npr3* than lira 12-h ( $P < .05$ ; Fig. 4C). The expression of endothelin-1 (*edn1*) decreased in response to lira treatment (Fig. 4D). Levels were more than 17-fold lower in lira

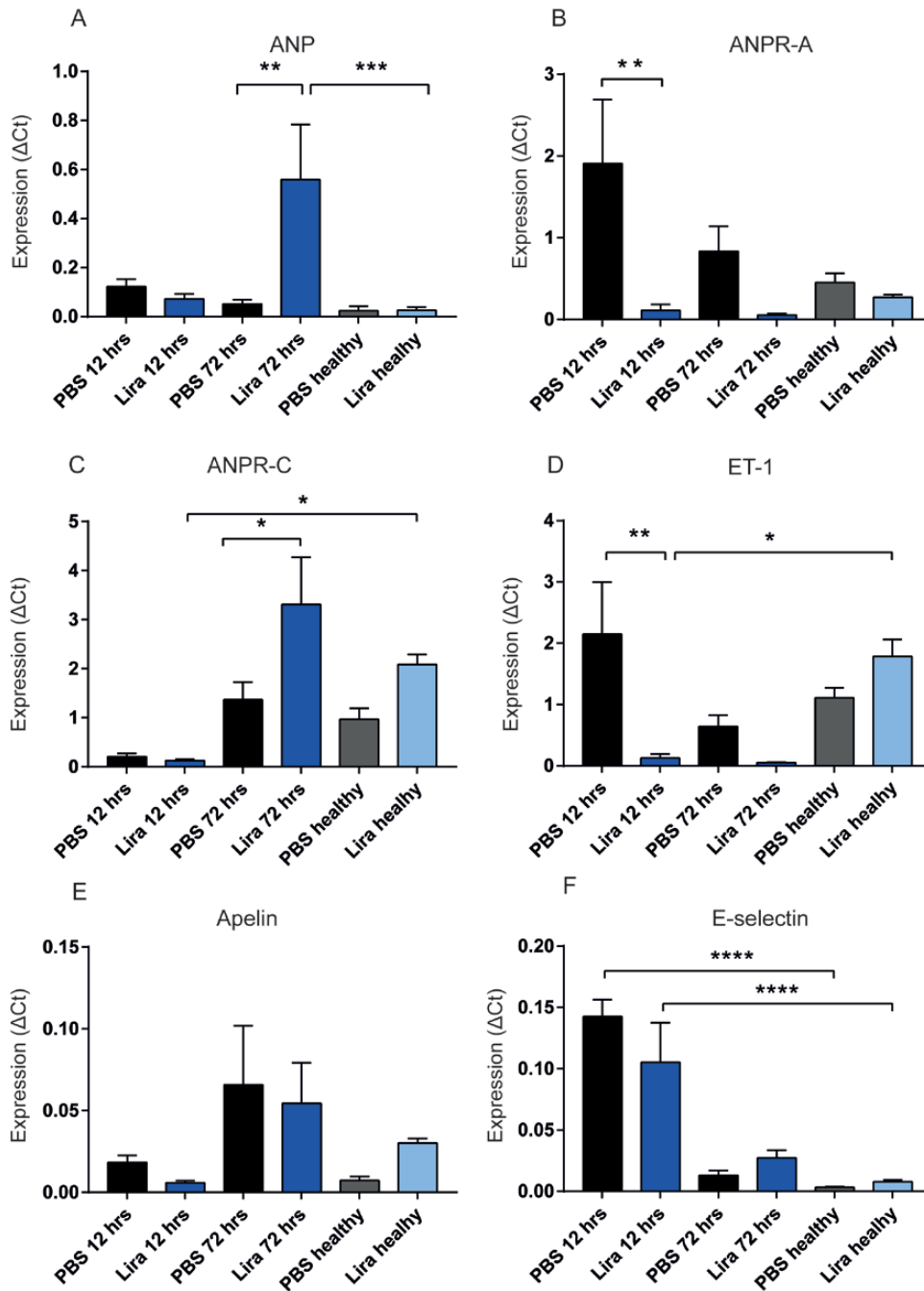


**Figure 4.** Gene expression analysis. All genes were normalized to the housekeeping gene *HPRT-1*. A, ANP (*nppa*); B, ANPR-A (*npr1*); C, ANP clearance receptor, ANPR-C (*npr3*); and D, endothelin-1, ET-1 (*edn1*). E, Apelin (*apl*). F, E-selectin (*sele*). *PBS healthy* and *lira healthy* refer to animals treated for 10 days with liraglutide or PBS, but with no induction of COPD. Data are expressed as means  $\pm$  SEM,  $n = 32$ . Statistics were analyzed using 1-way ANOVA followed by post hoc test comparing PBS and lira at 12 or 72 h \* $P < .05$ , \*\* $P < .01$ , \*\*\* $P < .001$ .

12-h vs PBS 12-h ( $P < .01$ ) and 16-fold lower than the healthy lira group. There was no significant difference between the lira and PBS groups regarding expression of *apl* and *sele* (Fig. 4D and 4F), but there was a significant increase in expression of *sele* in COPD mice at 12 hours compared to the healthy group ( $P < .001$ ).

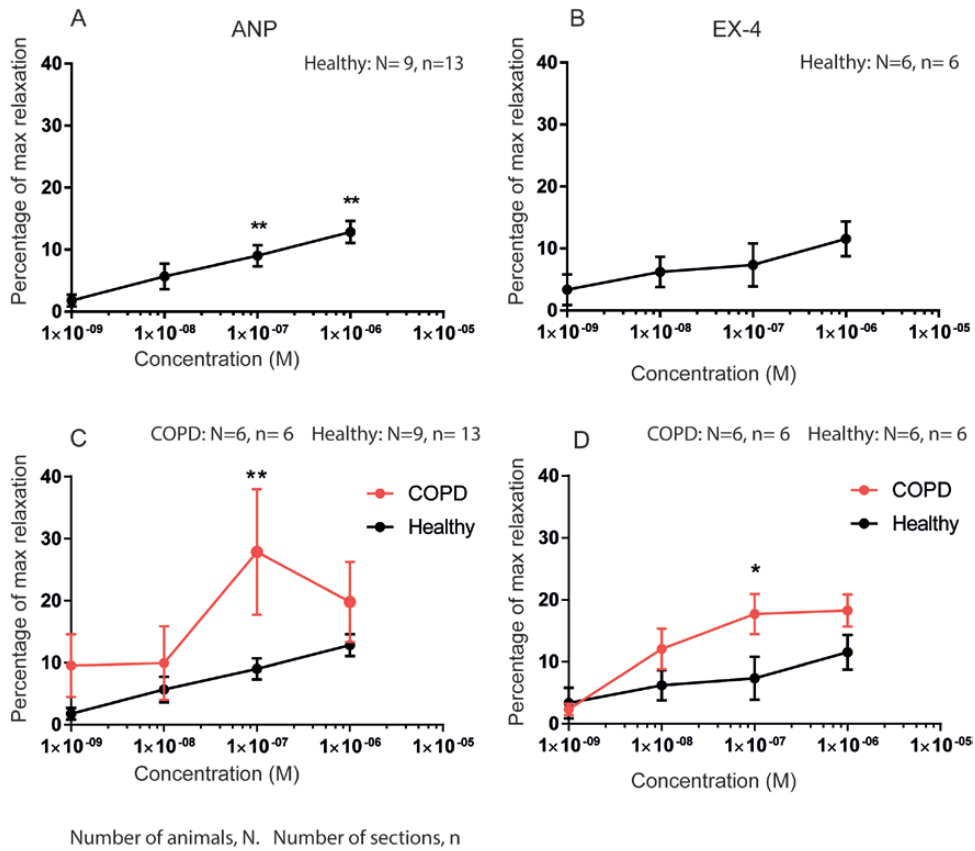


**Figure 5.** ANP and EX-4 both exerted bronchodilating effects on isolated bronchi of mice. Concentration-relaxation curves induced by ANP and EX-4 on bronchial smooth muscle tissue. Values are expressed relative to the maximal effect of SNP (0.1 mM), which was added at the end of the experiment. Data are shown as means  $\pm$  SEM. A, Relaxation induced by ANP (0.001-1 mM) in healthy mice. B, Relaxation induced by EX-4 (0.001-1 mM) in healthy mice. C, The effect of ANP on tissue from COPD mice compared to healthy mice. D, The effect of EX-4 on COPD mice compared to healthy mice. Data from A and B were analyzed by 1-way ANOVA followed by Bonferroni post hoc test comparing each concentration to 0.001 mM, which was considered as zero effect. Data from C and D were analyzed by 2-way ANOVA followed by Sidak post hoc test comparing the responses of COPD and healthy mice at each concentration. \* $P < .05$ , \*\* $P < .01$ .

### F. Atrial Natriuretic Peptide and Exendin-4 Both Exert Bronchodilating Effects on Isolated Mouse Bronchi

In healthy mice, significant relaxing effects of ANP were observed at 0.1  $\mu$ M and 1  $\mu$ M compared to 0.001  $\mu$ M, which was considered to have no effect ( $P < .01$ ) (Fig. 5A). At 1  $\mu$ M ANP-mediated dilation was  $12 \pm 2\%$  of  $R_{\max}$ . Ex-4 also showed bronchodilating effects (Fig. 5B), although to a lesser extent than ANP and with no significant difference between responses at increasing doses. The maximum response was achieved at 1  $\mu$ M with  $11 \pm 3\%$  of  $R_{\max}$ .

The maximal bronchodilating effect produced by ANP was  $28.6 \pm 8.9\%$  of  $R_{\max}$  at 0.1  $\mu$ M in bronchi from COPD mice, which was a 2-fold increase compared to bronchi from healthy mice (Fig. 5C). The COPD mice also showed a significantly greater response to EX-4, reaching a maximum at 0.1  $\mu$ M with  $17.7 \pm 3.3\%$  of  $R_{\max}$  corresponding to a 1.7-fold increase compared to the healthy mice ( $P < 0.5$ ) (Fig. 5E). A few of the sections did not respond to the peptides, and these were excluded from the data set. Data including these “nonresponders” are shown in Fig. 6. Sections that did not respond to SNP were discarded from the experiment.

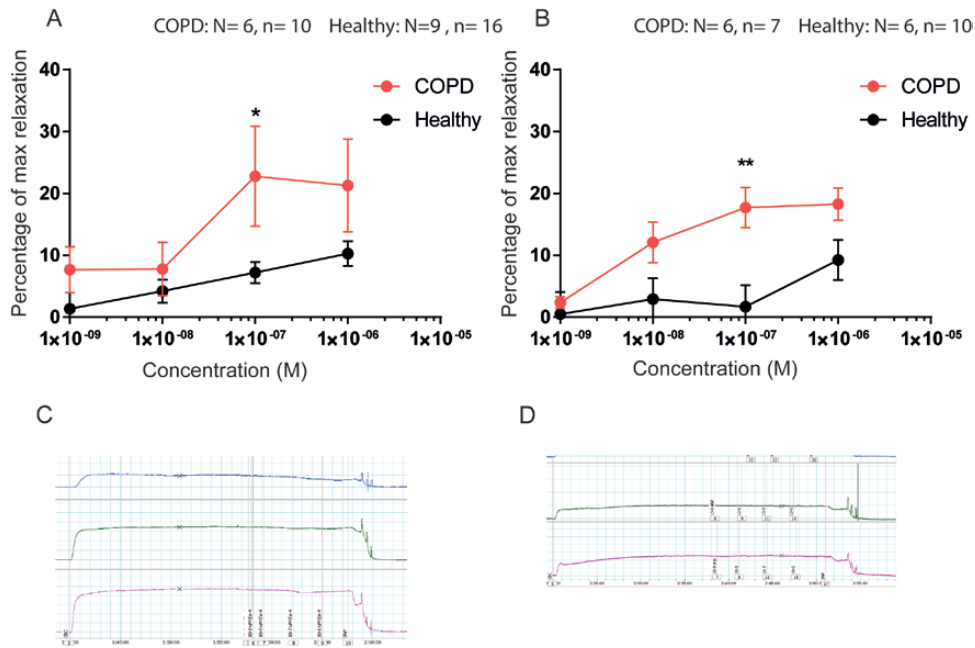


**Figure 6.** Direct effects of ANP and Ex-4 on smooth muscles of isolated mouse bronchi, including nonresponders. Concentration-relaxation curves induced by ANP and EX-4 on bronchial smooth muscle tissue. Relaxation values are expressed as a percentage of the relaxation seen with a maximally effective concentration of SNP (0.1 mM) added at the end of the experiment. Data are shown as means  $\pm$  SEM. A, The effect of ANP on tissue from COPD compared to healthy mice. B, The effect of EX-4 on COPD mice compared to healthy mice. C, Example of myograph signals from tissue sections responding to ANP and D, not responding to ANP, but to SNP.

### 3. Discussion

Because asthma and COPD prevalence is increased in individuals with obesity and type 2 diabetes (62, 63), and plasma GLP-1 concentrations are often decreased in these individuals (64, 65), we found it of interest to study whether endogenous GLP-1 could have protective functions in the pulmonary system. Previous studies have shown beneficial effects of GLP-1 analogues in different models of lung disease. Viby et al used a mouse model of obstructive pulmonary disease and showed that treatment with lira and EX-4 was able to decrease mortality rate and increase lung function by decreasing obstruction as measured by PenH (20). In a study of monocrotaline-induced pulmonary arterial hypertension, Lee and colleagues found that monocrotaline reduced endothelial nitric oxide (NO) synthase and thereby inhibited NO production in blood vessels. Lira treatment reversed this reduction. Additionally, lira inhibited ROCK signaling and ET-1 levels (24). In 2 independent studies of GLP-1 on isolated segments of pulmonary vasculature and trachea from the rat, there were minor dilatory effects on the vasculature, and this effect was endothelial and NO dependent (21, 66).

However, endogenous GLP-1 did not have apparent protective effects in our model of COPD when GLP-1 signaling was attenuated acutely by administration of EX-9 nor by receptor deletion (GLP-1R KO mice). However, we were able to confirm that lira decreased PenH and thereby reduced bronchoconstriction.

There were, nevertheless, marked differences in PenH values between the experiments. These differences could be at least partly related to interstrain differences between the mice used in the antagonist studies, obtained from a commercial vendor, and the GLP-1R KO mice and WT littermates representing an inbred strain. Indeed, studies have shown great variability with both interstrain and intrastrain phenotypic variation caused by genetic heterogeneity (67, 68).

For the present studies, we used a mouse model of COPD and evaluated the degree of disease by measuring lung function by PenH using unrestrained whole-body plethysmography. In humans, pulmonary function is estimated by spirometry using the Tiffeneau index (forced expiratory volume in 1 s/forced vital capacity [FEV<sub>1</sub>/FVC] ratio), a method that is not applicable in animals. The most reliable measurement of airway resistance and bronchial obstruction is through forced oscillation. This invasive technique is time consuming and terminal for the animals and incompatible with repeated measurements. Unrestrained whole-body plethysmography has been widely used to assess bronchial responsiveness in mouse disease models. PenH, which is based on changes in breathing patterns, is a dimensionless calculated measurement indicative of broncho-obstruction (49). This method has been criticized for being inadequate and an unreliable measurement of broncho-obstruction by some scientists (69-71), whereas others find it appropriate to use (49, 72-74), specifically in models of severe lung disease (75). Because we consider our model to be one of severe lung disease, we found it suitable for our studies. We found it more important that the animals were unrestrained and unanesthetized during our study period, thereby avoiding unnecessary stress that might be reflected in our results. Also, we were interested in longitudinal measurements that are not possible if using invasive measurements.

The decreased PenH values in the lira-treated group could to some extent reflect direct effects on the muscle tissue surrounding the bronchi, causing relief of constriction but might also be due to an indirect effect through attenuation of the inflammatory response. Indeed, several studies have shown that GLP-1 also has anti-inflammatory effects (43) in lung disease (19, 41, 42, 76, 77). To some extent our data support these findings.

Our histopathological score revealed less histological inflammation in the lira-treated group 12 hours after last LPS inhalation compared to PBS. Similarly, in a study of bleomycin-induced pulmonary fibrosis, Gou and colleagues found that lira decreased the number of macrophages and lymphocytes from bronchoalveolar lavage fluid. In that study, plasma concentrations of TNF- $\alpha$ , IL-6, and IL-1 $\beta$  were reduced with lira compared to placebo (19), whereas we were unable to detect any differences although the measured concentrations were within the detection and sensitivity range of the assay. On overexpression of GLP-1R in airway smooth muscle cells obtained from human biopsies, Sun and colleagues found decreased migration and proliferation as well as suppressed proinflammatory cytokines TNF- $\alpha$ , IL-4, and IL-1 $\beta$  (41). Whether these differences reflect interspecies variation, are a result of the supraphysiological expression of GLP-1R in the transfected cells, or linked to other differences between an in vivo and in vitro setup remains to be investigated further.

Although we did not find attenuation in levels of proinflammatory cytokines, our data confirm that lira treatment attenuated inflammation during the acute phase, 12 hours after the last LPS inhalation.

Part of our study aim was to investigate whether the beneficial effects of GLP-1 in lung disease were due to bronchodilatory effects elicited by stimulation of ANP secretion on GLP-1R activation. This hypothesis was inspired by the work of Kim et al from 2013 (12), showing that native GLP-1, EX-4, and lira all decreased blood pressure and increased natriuresis in hypertensive mice by mechanisms that were positively linked to increased plasma concentrations of ANP. Importantly, the beneficial effects were abolished in GLP-1R KO mice, suggesting that the ANP release was dependent on GLP-1R signaling. Later, the same authors carried out another study to investigate whether this translated to humans (78), but this did not appear to be the case.

Two other studies by another group arrived at a similar conclusion. Skov and colleagues found no increased levels of plasma proANP on native GLP-1 infusion in either healthy adult men or men with diabetes (79, 80). Following this study, the same group published another paper supporting the existence of a gut-ANP axis. Here they found increased levels of plasma ANP on different kinds of meal intake, but this study does not narrow down whether this effect may be mediated by GLP-1 (81). The data on the role of GLP-1 and ANP secretion in humans are, however, divergent and require further investigation because another

human study found that lira increased plasma concentrations of natriuretic peptides (ANP and BNP) after 12 weeks of treatment (82).

ANP is mainly secreted by the atrial cardiomyocytes but a few studies have reported secretion from the lung (33, 34). Unfortunately, it was not technically feasible for us to measure secretion of ANP in the present experimental in vivo models because reliable low-volume assays with sufficient sensitivity are not currently available. Also, plasma levels of ANP do not reveal from which organ it is secreted. Instead, we performed qPCR on lung tissue from mice subjected to our COPD model and healthy controls. Here we found a 10-fold increase in *nppa* transcripts in the lira group 72 hours after the last LPS inhalation.

Besides the increase in transcripts of *nppa* in the lira-treated group, we found an even greater increase in the transcription of the receptor for ANP, *npr1*. Unexpectedly, this was observed in the PBS-treated group. Also, we would expect to see the same difference between the 2 groups at 12 and 72 hours, which was not the case. We did, however, find a major improvement in Penh in the 12-h group treated with lira, and based on the lack of *nppa* expression our data do not support that the acute effect of GLP-1 is mediated by an upregulation of *nppa*. Interestingly, the expression of *npr3*, an ANP clearance receptor, was increased in the lira 72-h group, possibly as a response to the increased transcription of *nppa*.

We also measured *edn1* (ET-1). ET-1 is a peptide with bronchoconstricting properties, and elevated levels are found in patients with asthma and eosinophilic infiltrations as well as in patients with pulmonary hypertension (83). We found an 18-fold and 13-fold decrease in *edn1* levels in the lira 12-h and 72-h group, respectively, compared to the PBS groups. These findings are supported by a study by Lee et al, who found a decrease in ET-1 levels on lira treatment in a rat model of pulmonary hypertension (24). In another study, it was found that ANP inhibited the expression of ET-1 in cardiac fibroblasts through a GATA-4-dependent mechanism (84). Isono and colleagues found that ANP inhibited ET-1 activation of c-Jun NH<sub>2</sub>-terminal kinase in glomerular mesangial cells (85). Apparently, both lira and ANP have been found to inhibit the expression of ET-1. Our data do not reveal whether the decrease is due to a direct effect of lira or an indirect effect of the increased levels of ANP induced by lira, but *edn1* upregulation could be the mediator of the reduced PenH in the acute phase.

Based on these findings we can conclude that ANP in the lung, at the transcriptional level, is increased on lira treatment. Moreover, this effect is more pronounced after reaching maximal constriction.

Bronchodilating effects of ANP are not novel. Several studies carried out in the 1990s showed that ANP has direct bronchodilatory effects on isolated bronchial tissue from guinea pig, rabbit, and cow (37, 40, 86) but the effect on mouse tissue has not been reported before. Consistent with the previous findings, we observed a bronchodilatory effect of ANP surprisingly also an effect of GLP-1. However, the responses to EX-4 varied greatly between animals, with some responding robustly and others not responding at all (nonresponders: 4/10). The responses to ANP also varied (nonresponders: 3/16) but not as much as with EX-4. Varying responses to ANP in bronchodilation were also observed by Hulks et al in asthmatic patients, among whom “some responded nicely and others not at all” (40).

Our gene expression data revealed that the expression of ANPR-A was upregulated under the disease state in the PBS-treated group. Therefore, we investigated whether this translated into increased sensitivity to ANP and EX-4 with regards to bronchodilatory effects. Indeed, response to ANP was 2.2-fold higher in COPD mice compared to healthy mice, and for EX-4 the response was 1.7-fold higher in COPD mice.

Taken together this shows that ANP and EX-4 both have direct bronchodilating effects, although the effect of ANP was more pronounced than that of EX-4. Moreover, these effects were significantly increased in sick animals, which is in line with the patterns of gene expression for the ANP receptor. Although this needs further investigation, our data could indicate that the sick lung compensates by increasing its expression of ANPR-A, resulting in increased sensitivity to the potentially increased levels of ANP and increased bronchodilating effects of both peptides.

## 4. Conclusion

We were unable to show that endogenous GLP-1 plays a protective role in a mouse model of COPD, but exogenous doses of lira were indeed protective. Lira attenuated inflammation, but not the levels of proinflammatory cytokines. Expression of *nppa* was increased under disease states of the lung and was further increased on treatment with lira. ANP and to a lesser extent EX-4 have bronchodilatory properties that are more pronounced in COPD mice. *Edn1* expression was decreased either as a direct consequence of lira or indirectly through the increase in ANP. The role of GLP-1 in lung disease still warrants more investigation, including further studies of the link between GLP-1 and ANP. Our findings support studies of a potential role for GLP-1 analogues in the treatment for patients with acute exacerbation of COPD.

## Acknowledgments

We thank Reidar Albrechtsen for valuable input and emphysema scoring.

**Financial Support:** This work was supported by grants from the Independent Research Fund Denmark, Danielsen Foundation, A.P. Møller Foundation, and Wedell-Wedellsborg Foundation. The funding sources had no influence on the trial design or data collection, management, analysis, or reporting.

**Author Contributions:** E.B.M. and H.K. planned and conducted the experiments, analyzed and interpreted the data, and drafted the manuscript. B.S. conducted the isolated perfused pancreas experiment. J.H. and S.G.M. contributed to the gene expression analyses and interpretation of the results. J.A.W. contributed to the generation of the GLP-1R KO mice. C.M.S. contributed to myograph studies. J.J.H. contributed to data interpretation and manuscript preparation. All authors commented on and approved the final version of the manuscript.

## Additional Information

**Correspondence:** Hannelouise Kissow, MD, PhD, Department of Biomedical Sciences, Faculty of Health and Medical Sciences, University of Copenhagen, Blegdamsvej 3, DK-2200 Copenhagen N, Denmark. E-mail: [kissow@sund.ku.dk](mailto:kissow@sund.ku.dk).

**Disclosure Summary:** The authors have nothing to disclose.

---

## References

1. Orskov C, Wettergren A, Holst JJ. Secretion of the incretin hormones glucagon-like peptide-1 and gastric inhibitory polypeptide correlates with insulin secretion in normal man throughout the day. *Scand J Gastroenterol*. 1996;**31**(7):665–670.
2. Vilsbøll T, Krarup T, Sonne J, et al. Incretin secretion in relation to meal size and body weight in healthy subjects and people with type 1 and type 2 diabetes mellitus. *J Clin Endocrinol Metab*. 2003;**88**(6):2706–2713.
3. Holst JJ. The physiology of glucagon-like peptide 1. *Physiol Rev*. 2007;**87**(4):1409–1439.
4. Wilding JPH. Medication use for the treatment of diabetes in obese individuals. *Diabetologia*. 2018;**61**(2):265–272.
5. Seufert J, Gallwitz B. The extra-pancreatic effects of GLP-1 receptor agonists: a focus on the cardiovascular, gastrointestinal and central nervous systems. *Diabetes Obes Metab*. 2014;**16**(8):673–688.
6. Jensen EP, Poulsen SS, Kissow H, et al. Activation of GLP-1 receptors on vascular smooth muscle cells reduces the autoregulatory response in afferent arterioles and increases renal blood flow. *Am J Physiol Renal Physiol*. 2015;**308**(8):F867–F877.
7. Zander M, Madsbad S, Madsen JL, Holst JJ. Effect of 6-week course of glucagon-like peptide 1 on glycaemic control, insulin sensitivity, and beta-cell function in type 2 diabetes: a parallel-group study. *Lancet*. 2002;**359**(9309):824–830.
8. Dunphy JL, Taylor RG, Fuller PJ. Tissue distribution of rat glucagon receptor and GLP-1 receptor gene expression. *Mol Cell Endocrinol*. 1998;**141**(1-2):179–186.

9. Bullock BP, Heller RS, Habener JF. Tissue distribution of messenger ribonucleic acid encoding the rat glucagon-like peptide-1 receptor. *Endocrinology*. 1996;**137**(7):2968–2978.
10. Campos RV, Lee YC, Drucker DJ. Divergent tissue-specific and developmental expression of receptors for glucagon and glucagon-like peptide-1 in the mouse. *Endocrinology*. 1994;**134**(5):2156–2164.
11. Pyke C, Heller RS, Kirk RK, et al. GLP-1 receptor localization in monkey and human tissue: novel distribution revealed with extensively validated monoclonal antibody. *Endocrinology*. 2014;**155**(4):1280–1290.
12. Kim M, Platt MJ, Shibasaki T, et al. GLP-1 receptor activation and Epac2 link atrial natriuretic peptide secretion to control of blood pressure. *Nat Med*. 2013;**19**(5):567–575.
13. Oztay F, Sancar-Bas S, Gezginci-Oktayoglu S, Ercin M, Bolkent S. Exendin-4 partly ameliorates hyperglycemia-mediated tissue damage in lungs of streptozotocin-induced diabetic mice. *Peptides*. 2018;**99**:99–107.
14. Kanse SM, Kreymann B, Ghatei MA, Bloom SR. Identification and characterization of glucagon-like peptide-1 7-36 amide-binding sites in the rat brain and lung. *FEBS Lett*. 1988;**241**(1-2):209–212.
15. Richter G, Göke R, Göke B, Schmidt H, Arnold R. Characterization of glucagon-like peptide-I(7-36) amide receptors of rat lung membranes by covalent cross-linking. *FEBS Lett*. 1991;**280**(2):247–250.
16. Richter G, Göke R, Göke B, Arnold R. Characterization of receptors for glucagon-like peptide-1(7-36) amide on rat lung membranes. *FEBS Lett*. 1990;**267**(1):78–80.
17. Wei Y, Mojsov S. Tissue-specific expression of the human receptor for glucagon-like peptide-I: brain, heart and pancreatic forms have the same deduced amino acid sequences. *FEBS Lett*. 1995;**358**(3):219–224.
18. Hassan M, Eskilsson A, Nilsson C, et al. In vivo dynamic distribution of 131I-glucagon-like peptide-1 (7-36) amide in the rat studied by gamma camera. *Nucl Med Biol*. 1999;**26**(4):413–420.
19. Gou S, Zhu T, Wang W, Xiao M, Wang XC, Chen ZH. Glucagon like peptide-1 attenuates bleomycin-induced pulmonary fibrosis, involving the inactivation of NF-κB in mice. *Int Immunopharmacol*. 2014;**22**(2):498–504.
20. Viby NE, Isidor MS, Buggeskov KB, Poulsen SS, Hansen JB, Kissow H. Glucagon-like peptide-1 (GLP-1) reduces mortality and improves lung function in a model of experimental obstructive lung disease in female mice. *Endocrinology*. 2013;**154**(12):4503–4511.
21. Golpon HA, Puechner A, Welte T, Wichert PV, Feddersen CO. Vasorelaxant effect of glucagon-like peptide-(7-36)amide and amylin on the pulmonary circulation of the rat. *Regul Pept*. 2001;**102**(2-3):81–86.
22. Zhou F, Zhang Y, Chen J, Hu X, Xu Y. Liraglutide attenuates lipopolysaccharide-induced acute lung injury in mice. *Eur J Pharmacol*. 2016;**791**:735–740.
23. Zhu T, Wu XL, Zhang W, Xiao M. Glucagon like peptide-1 (GLP-1) modulates OVA-induced airway inflammation and mucus secretion involving a protein kinase A (PKA)-dependent nuclear factor-κB (NF-κB) signaling pathway in mice. *Int J Mol Sci*. 2015;**16**(9):20195–20211.
24. Lee MY, Tsai KB, Hsu JH, Shin SJ, Wu JR, Yeh JL. Liraglutide prevents and reverses monocrotaline-induced pulmonary arterial hypertension by suppressing ET-1 and enhancing eNOS/sGC/PKG pathways. *Sci Rep*. 2016;**6**:31788.
25. Lim SB, Rubinstein I, Sadikot RT, Artwohl JE, Önyüksel H. A novel peptide nanomedicine against acute lung injury: GLP-1 in phospholipid micelles. *Pharm Res*. 2011;**28**(3):662–672.
26. Vara E, Arias-Díaz J, Garcia C, Balibrea JL, Blázquez E. Glucagon-like peptide-1(7-36) amide stimulates surfactant secretion in human type II pneumocytes. *Am J Respir Crit Care Med*. 2001;**163**(4):840–846.
27. Potter LR, Yoder AR, Flora DR, Antos LK, Dickey DM. Natriuretic peptides: their structures, receptors, physiologic functions and therapeutic applications. *Handb Exp Pharmacol*. 2009;**191**:341–366.
28. Kumar R, Cartledge WA, Lincoln TM, Pandey KN. Expression of guanylyl cyclase-A/atrial natriuretic peptide receptor blocks the activation of protein kinase C in vascular smooth muscle cells. Role of cGMP and cGMP-dependent protein kinase. *Hypertension*. 1997;**29**(1 Pt 2):414–421.
29. Newton-Cheh C, Larson MG, Vasan RS, et al. Association of common variants in NPPA and NPPB with circulating natriuretic peptides and blood pressure. *Nat Genet*. 2009;**41**(3):348–353.
30. Baxter GF. The natriuretic peptides. *Basic Res Cardiol*. 2004;**99**(2):71–75.
31. Werner F, Kojonazarov B, Gaßner B, et al. Endothelial actions of atrial natriuretic peptide prevent pulmonary hypertension in mice. *Basic Res Cardiol*. 2016;**111**(2):22.
32. Bianchi C, Gutkowska J, Garcia R, Thibault G, Genest J, Cantin M. Localization of 125I-atrial natriuretic factor (ANF)-binding sites in rat renal medulla. A light and electron microscope autoradiographic study. *J Histochem Cytochem*. 1987;**35**(2):149–153.
33. Gutkowska J, Nemer M. Structure, expression, and function of atrial natriuretic factor in extraatrial tissues. *Endocr Rev*. 1989;**10**(4):519–536.



34. Gutkowska J, Cantin M, Genest J, Sirois P. Release of immunoreactive atrial natriuretic factor from the isolated perfused rat lung. *FEBS Lett.* 1987;**214**(1):17–20.
35. Hamel R, Ford-Hutchinson AW. Relaxant profile of synthetic atrial natriuretic factor on guinea-pig pulmonary tissues. *Eur J Pharmacol.* 1986;**121**(1):151–155.
36. O'Donnell M, Garippa R, Welton AF. Relaxant activity of atriopeptins in isolated guinea pig airway and vascular smooth muscle. *Peptides.* 1985;**6**(4):597–601.
37. Ishii K, Murad F. ANP relaxes bovine tracheal smooth muscle and increases cGMP. *Am J Physiol.* 1989;**256**(3 Pt 1):C495–C500.
38. Eison HB, Rosen MJ, Phillips RA, Krakoff LR. Determinants of atrial natriuretic factor in the adult respiratory distress syndrome. *Chest.* 1988;**94**(5):1040–1045.
39. Skwarski K, Lee M, Turnbull L, MacNee W. Atrial natriuretic peptide in stable and decompensated chronic obstructive pulmonary disease. *Thorax.* 1993;**48**(7):730–735.
40. Hulks G, Jardine A, Connell JM, Thomson NC. Bronchodilator effect of atrial natriuretic peptide in asthma. *BMJ.* 1989;**299**(6707):1081–1082.
41. Sun YH, He L, Yan MY, et al. Overexpression of GLP-1 receptors suppresses proliferation and cytokine release by airway smooth muscle cells of patients with chronic obstructive pulmonary disease via activation of ABCA1. *Mol Med Rep.* 2017;**16**(1):929–936.
42. Nguyen DV, Linderholm A, Haczku A, Kenyon N. Glucagon-like peptide 1: a potential anti-inflammatory pathway in obesity-related asthma. *Pharmacol Ther.* 2017;**180**:139–143.
43. Insuela DBR, Carvalho VF. Glucagon and glucagon-like peptide-1 as novel anti-inflammatory and immunomodulatory compounds. *Eur J Pharmacol.* 2017;**812**:64–72.
44. International Knockout Mouse Consortium. MGI download of modified allele data from IKMC and creation of new knockout alleles. MGI website. <http://www.informatics.jax.org/allele/MGI:5692922#references>. 2014.
45. Schwenk F, Baron U, Rajewsky K. A cre-transgenic mouse strain for the ubiquitous deletion of loxP-flanked gene segments including deletion in germ cells. *Nucleic Acids Res.* 1995;**23**(24):5080–5081.
46. Svendsen B, Larsen O, Gabe MBN, et al. Insulin secretion depends on intra-islet glucagon signaling. *Cell Rep.* 2018;**25**(5):1127–1134.e2.
47. The Antibody Registry. RRID:AB\_2814792. The Antibody Registry website. [https://antibodyregistry.org/search?q=AB\\_2814792](https://antibodyregistry.org/search?q=AB_2814792).
48. Brand CL, Jørgensen PN, Knigge U, et al. Role of glucagon in maintenance of euglycemia in fed and fasted rats. *Am J Physiol.* 1995;**269**(3 Pt 1):E469–E477.
49. Hamelmann E, Schwarze J, Takeda K, et al. Noninvasive measurement of airway responsiveness in allergic mice using barometric plethysmography. *Am J Respir Crit Care Med.* 1997;**156**(3 Pt 1):766–775.
50. de Siqueira AL, Russo M, Steil AA, Facincone S, Mariano M, Jancar S. A new murine model of pulmonary eosinophilic hypersensitivity: contribution to experimental asthma. *J Allergy Clin Immunol.* 1997;**100**(3):383–388.
51. Facincone S, De Siqueira AL, Jancar S, Russo M, Barbuto JA, Mariano M. A novel murine model of late-phase reaction of immediate hypersensitivity. *Mediators Inflamm.* 1997;**6**(2):127–133.
52. Rolin B, Larsen MO, Gotfredsen CF, et al. The long-acting GLP-1 derivative NN2211 ameliorates glycemia and increases beta-cell mass in diabetic mice. *Am J Physiol Endocrinol Metab.* 2002;**283**(4):E745–E752.
53. Göke R, Fehmann HC, Linn T, et al. Exendin-4 is a high potency agonist and truncated exendin-(9-39)-amide an antagonist at the glucagon-like peptide 1-(7-36)-amide receptor of insulin-secreting beta-cells. *J Biol Chem.* 1993;**268**(26):19650–19655.
54. Malhotra R, Singh L, Eng J, Raufman JP. Exendin-4, a new peptide from *Heloderma suspectum* venom, potentiates cholecystokinin-induced amylase release from rat pancreatic acini. *Regul Pept.* 1992;**41**(2):149–156.
55. The Antibody Registry. RRID:AB\_2618101. The Antibody Registry website. [https://antibodyregistry.org/search?q=AB\\_2618101](https://antibodyregistry.org/search?q=AB_2618101).
56. Jensen EP, Poulsen SS, Kissow H, et al. Activation of GLP-1 receptors on vascular smooth muscle cells reduces the autoregulatory response in afferent arterioles and increases renal blood flow. *Am J Physiol Renal Physiol.* 2015;**308**(8):F867–F877.
57. Jensen CB, Pyke C, Rasch MG, Dahl AB, Knudsen LB, Secher A. Characterization of the glucagonlike peptide-1 receptor in male mouse brain using a novel antibody and in situ hybridization. *Endocrinology.* 2018;**159**(2):665–675.
58. The Antibody Registry. RRID:AB\_1523910. The Antibody Registry website. [https://antibodyregistry.org/search?q=AB\\_1523910](https://antibodyregistry.org/search?q=AB_1523910).

59. Zeldin DC, Wohlford-Lenane C, Chulada P, et al. Airway inflammation and responsiveness in prostaglandin H synthase-deficient mice exposed to bacterial lipopolysaccharide. *Am J Respir Cell Mol Biol*. 2001;**25**(4):457–465.
60. Ghiasi SM, Krogh N, Tyrberg B, Mandrup-Poulsen T. The No-Go and Nonsense-Mediated RNA decay pathways are regulated by inflammatory cytokines in insulin-producing cells and human islets and determine  $\beta$ -cell insulin biosynthesis and survival. *Diabetes*. 2018;**67**(10):2019–2037.
61. Liu JQ, Yang D, Folz RJ. A novel bronchial ring bioassay for the evaluation of small airway smooth muscle function in mice. *Am J Physiol Lung Cell Mol Physiol*. 2006;**291**(2):L281–L288.
62. Leone N, Courbon D, Thomas F, et al. Lung function impairment and metabolic syndrome: the critical role of abdominal obesity. *Am J Respir Crit Care Med*. 2009;**179**(6):509–516.
63. Chatila WM, Thomashow BM, Minai OA, Criner GJ, Make BJ. Comorbidities in chronic obstructive pulmonary disease. *Proc Am Thorac Soc*. 2008;**5**(4):549–555.
64. Knop FK, Aaboe K, Vilsbøll T, et al. Impaired incretin effect and fasting hyperglucagonaemia characterizing type 2 diabetic subjects are early signs of dysmetabolism in obesity. *Diabetes Obes Metab*. 2012;**14**(6):500–510.
65. Holst JJ, Knop FK, Vilsbøll T, Krarup T, Madsbad S. Loss of incretin effect is a specific, important, and early characteristic of type 2 diabetes. *Diabetes Care*. 2011;**34**(Suppl 2):S251–S257.
66. Richter G, Feddersen O, Wagner U, Barth P, Göke R, Göke B. GLP-1 stimulates secretion of macromolecules from airways and relaxes pulmonary artery. *Am J Physiol*. 1993;**265**(4 Pt 1):L374–L381.
67. Löscher W, Ferland RJ, Ferraro TN. The relevance of inter- and intrastrain differences in mice and rats and their implications for models of seizures and epilepsy. *Epilepsy Behav*. 2017;**73**:214–235.
68. Festing MF. Genetic variation in outbred rats and mice and its implications for toxicological screening. *J Exp Anim Sci*. 1993;**35**(5-6):210–220.
69. Bates J, Irvin C, Brusasco V, et al. The use and misuse of Penh in animal models of lung disease. *Am J Respir Cell Mol Biol*. 2004;**31**(3):373–374.
70. Frazer DG, Reynolds JS, Jackson MC. Determining when enhanced pause (Penh) is sensitive to changes in specific airway resistance. *J Toxicol Environ Health A*. 2011;**74**(5):287–295.
71. Lundblad LK, Irvin CG, Adler A, Bates JH. A reevaluation of the validity of unrestrained plethysmography in mice. *J Appl Physiol (1985)*. 2002;**93**(4):1198–1207.
72. Vanoirbeek JA, Mandervelt C, Cunningham AR, et al. Validity of methods to predict the respiratory sensitizing potential of chemicals: a study with a piperidinyl chlorotriazine derivative that caused an outbreak of occupational asthma. *Toxicol Sci*. 2003;**76**(2):338–346.
73. De Vooght V, Cruz MJ, Haenen S, et al. Ammonium persulfate can initiate an asthmatic response in mice. *Thorax*. 2010;**65**(3):252–257.
74. Lomask M. Further exploration of the Penh parameter. *Exp Toxicol Pathol*. 2006;**57**(Suppl 2):13–20.
75. Verheijden KA, Henricks PA, Redegeld FA, Garssen J, Folkerts G. Measurement of airway function using invasive and non-invasive methods in mild and severe models for allergic airway inflammation in mice. *Front Pharmacol*. 2014;**5**:190.
76. Huang J, Yi H, Zhao C, et al. Glucagon-like peptide-1 receptor (GLP-1R) signaling ameliorates dysfunctionality in COPD patients. *Int J Chron Obstruct Pulmon Dis*. 2018;**13**:3191–3202.
77. Zhu T, Li C, Zhang X, et al. GLP-1 analogue liraglutide enhances SP-A expression in LPS-induced acute lung injury through the TTF-1 signaling pathway. *Mediators Inflamm*. 2018;**2018**:3601454.
78. Lovshin JA, Barnie A, DeAlmeida A, Logan A, Zinman B, Drucker DJ. Liraglutide promotes natriuresis but does not increase circulating levels of atrial natriuretic peptide in hypertensive subjects with type 2 diabetes. *Diabetes Care*. 2015;**38**(1):132–139.
79. Skov J, Holst JJ, Gøtze JP, Frøkiær J, Christiansen JS. Glucagon-like peptide-1: effect on pro-atrial natriuretic peptide in healthy males. *Endocr Connect*. 2014;**3**(1):11–16.
80. Skov J, Pedersen M, Holst JJ, et al. Short-term effects of liraglutide on kidney function and vasoactive hormones in type 2 diabetes: a randomized clinical trial. *Diabetes Obes Metab*. 2016;**18**(6):581–589.
81. Sonne DP, Terzic D, Knop FK, Goetze JP. Postprandial plasma concentrations of proANP in patients with type 2 diabetes and healthy controls. *Clin Chem*. 2017;**63**(5):1040–1041.
82. Li CJ, Yu Q, Yu P, et al. Changes in liraglutide-induced body composition are related to modifications in plasma cardiac natriuretic peptides levels in obese type 2 diabetic patients. *Cardiovasc Diabetol*. 2014;**13**:36.
83. Fagan KA, McMurtry IF, Rodman DM. Role of endothelin-1 in lung disease. *Respir Res*. 2001;**2**(2):90–101.
84. Glenn DJ, Rahmutula D, Nishimoto M, Liang F, Gardner DG. Atrial natriuretic peptide suppresses endothelin gene expression and proliferation in cardiac fibroblasts through a GATA4-dependent mechanism. *Cardiovasc Res*. 2009;**84**(2):209–217.

85. Isono M, Haneda M, Maeda S, Omatsu-Kanbe M, Kikkawa R. Atrial natriuretic peptide inhibits endothelin-1-induced activation of JNK in glomerular mesangial cells. *Kidney Int.* 1998;**53**(5):1133–1142.
86. Mizuguchi M, Myo S, Fujimura M. Bronchoprotective effects of atrial natriuretic peptide against propranolol-induced bronchoconstriction after allergic reaction in guinea pigs. *Clin Exp Allergy.* 2000;**30**(3):439–444.